A DISCRETE SPECTRAL EVOLUTION MODEL FOR NONLINEAR WAVES OVER 2D TOPOGRAPHY

T. T. JANSSEN*[,1], T. H. C. HERBERS[2] AND J. A. BATTJES[1]

[1] *Faculty of Civil Engineering and Geosciences*
Delft University of Technology
Stevinweg 1, 2628 CN Delft, The Netherlands

[2] *Department of Oceanography, Naval Postgraduate School*
Monterey, California, 93943-5122, USA

A discrete spectral evolution model is presented suitable for the propagation of multi-directional wave fields over weakly two-dimensional topography. A coupled set of amplitude evolution equations is derived that includes the combined effects of wave-wave and wave-bottom interactions in deep-intermediate water depth. A heuristic extension to shallow water is given that describes quadratic wave-wave interactions without restriction on the resonance mismatch. Comparisons to experimental data demonstrate that the model accurately describes the effects of: 1) wave refraction and diffraction by topography with considerable two-dimensional features, and 2) harmonic generation in focal regions. A full account of the theory, including cubic wave-wave interactions and a rigorous treatment of the shallow water limit is given in Janssen *et al.* (2004).

1. Introduction

Waves advancing into shallow coastal areas and on beaches transform owing primarily to refraction (see e.g. Munk & Traylor , 1947) and near-resonant, quadratic, wave-wave interactions involving triplets of wave components. Super-harmonic interactions transform near-symmetrical waves to the characteristic skewed, pitched-forward shapes of waves observed on beaches and cause the occurrence of multi-crest wave trains behind submerged obstacles (see e.g. Byrne, 1969). Sub-harmonic interactions induce radiation of long wave motion in the nearshore region, generally referred to by the collective name 'surf beat', coined by its pioneering observer Munk (1949). These effects are recognized as major factors in the study of nearshore morpho-

*Corresponding author, email: t.t.janssen@citg.tudelft.nl

logical evolution (e.g. Boczar-Karakiewiczji & Davidson-Arnott, 1987) and of paramount importance in the design of coastal structures and harbors.

Great advances have been made in modeling nonlinear surface waves in coastal areas using coupled amplitude evolution equations. These models are either based on Boussinesq theory (e.g. Freilich & Guza, 1984; Madsen & Sørensen, 1993; Herbers & Burton, 1997) or fully dispersive theory, suitable for uni- or multi-directional waves over alongshore-uniform topography (e.g. Agnon *et al.*, 1993; Sheremet, 1996; Eldeberky & Madsen, 1999) and small-angle wave propagation over two-dimensional topography (e.g. Kaihatu & Kirby, 1995; Tang & Ouellet, 1997). In general, the models based on fully-dispersive theory include full dispersion in the linear terms and the nonlinear interaction coefficient but retain the premise of near-resonance. The latter restriction was removed by Bredmose *et al.* (2002) who apply suitable boundary conditions on a general solution to the Laplace equation in the form of infinite expansions of trigonometric functions (see also Madsen & Schäffer, 1998; Rayleigh, 1876) for unidirectional waves over one-dimensional bathymetry. Based on a WKB expansion and fully dispersive theory, Janssen *et al.* (2004) (JHB hereafter) derive an evolution equation for multi-directional waves over a weakly two-dimensional topography (see also Suh *et al.*, 1990) that allows for arbitrary resonance mismatch in the quadratic interactions and includes cubic wave-nonlinearities.

The present work presents an outline of the derivation detailed in JHB. In contrast to JHB we will 1) consider solely periodic wave motion, 2) omit most of the algebraic details, and 3) do not consider cubic wave-wave interactions. The approach in dealing with two-dimensional bathymetry follows closely the work by Suh *et al.* (1990) but differs from the outset due to the fact that: 1) we apply an alternative scaling so that the effects of quadratic (rather than the cubic) wave-wave interactions take place at the order of the bottom slopes, 2) the present model includes multi-frequency (irregular) wave fields and attendant harmonic generation in shallow water; on a more detailed level the derivation differs due to an alternative treatment of intermediate results, which is not discussed further here but addressed in JHB.

In §2 we discuss the general theory, the treatment of the two-dimensional bathymetry and wave field decomposition. The main result, a transport equation for the (complex) amplitudes of a wave field propagating over 2D bathymetry, including the effects of quadratic interactions for arbitrary resonance mismatch is presented in §3. A comparison to experimental data is included in §4 and the main findings and conclusions are given in §5.

2. Theoretical approach

The starting point of our derivation is the governing set of equations for irrotational flow of an incompressible, inviscid fluid:

$$\nabla^2\Phi + \Phi_{zz} = 0, \qquad \forall z \in \mathcal{D} \tag{1a}$$

$$\Phi_z + \nabla h \cdot \nabla\Phi = 0, \qquad z = -h(x,y) \tag{1b}$$

$$\Phi_{tt} + g\Phi_z + \mathcal{L}\left\{|\nabla\Phi|^2 + (\Phi_z)^2\right\} = 0, \qquad z = \eta(x,y,t) \tag{1c}$$

$$g\eta + \Phi_t + \frac{1}{2}\left(|\nabla\Phi|^2 + (\Phi_z)^2\right) = 0. \qquad z = \eta(x,y,t) \tag{1d}$$

Here Φ is a velocity potential function, g denotes gravitational acceleration, $\nabla \equiv \langle \partial_x, \partial_y \rangle$, where ∂_x is a shorthand for partial differentiation with respect to the subscript and the operator $\mathcal{L} \equiv \left[\partial_t + \frac{1}{2}\nabla\Phi \cdot \nabla + \frac{1}{2}\Phi_z\partial_z\right]$. We use a Cartesian frame of reference with its origin at the undisturbed free surface of the fluid; x and y denote the two horizontal coordinates and z corresponds to the vertical coordinate, positive pointing upward. The condition (1c) follows from combining the kinematic and dynamic free surface boundary conditions while assuming a constant atmospheric pressure (see e.g. Phillips, 1977, §3.1).

2.1. *Wave field decomposition for weak 2DH approximation*

We consider the description of weakly nonlinear surface waves over weakly two-dimensional bathymetry; the latter is considered one-dimensional to leading order with slow variations in its principal direction superposed by a two-dimensional perturbation, written as:

$$h(\mathbf{x}) = \overline{h}(x) - \widetilde{h}(\mathbf{x}). \tag{2}$$

Without loss of generality, we let the principal and lateral direction coincide with x and y respectively and since we are particularly interested in the description of waves propagating into a shallow coastal area from intermediate water depth, we refer to x as the cross-shore and y as the alongshore direction. In (2), $\overline{h}(x)$ represents a laterally averaged depth and $\widetilde{h} = \overline{h} - h$, the two dimensional residue.

The magnitude of the residual depth, $\widetilde{h}$ is governed by

$$O(\gamma) = O(\frac{\widetilde{h}}{\overline{h}}) \ll 1. \tag{3}$$

The spatial variation of the bathymetry is small over distances $O(k_0^{-1})$ – k_0 being a characteristic wavenumber of the wave motion – which is made explicit by the parameter

$$O(\beta) = O(\frac{\partial_x \overline{h}}{k_0 \overline{h}}) = O(\frac{\partial_x \widetilde{h}}{k_0 \overline{h}}) = O(\frac{\partial_y \widetilde{h}}{k_0 \overline{h}}) \ll 1. \tag{4}$$

The nonlinearity of the wave field is governed by the small parameter ϵ, where $\epsilon \equiv a_0/L_v \ll 1$; here a_0 and L_v denote a characteristic amplitude of the surface elevation and a representative vertical length scale respectively. The relative magnitudes of these small parameters are taken as

$$O(\epsilon) = O(\beta) = O(\gamma^2) \tag{5}$$

The amplitude of the topography (γ) is introduced here at a lower order than the nonlinearity (ϵ) to accurately resolve wave propagation over shallow submerged bathymetry features such as banks and shoals that are common in many coastal areas. Further, the scaling of eqs. (4) and (5) implies that the characteristic length scale of the 2D topography is long compared with the surface wavenumber, which excludes the modeling of back-scattering of waves (induced by bottom undulations of about half the surface wavelength), consistent with earlier studies of wave scattering from natural continental shelf topography (Ardhuin & Herbers, 2002).

The set (1) is solved by applying a perturbation expansion of the surface elevation and velocity potential in terms of the small parameter γ. The (leading-order) alongshore-uniform bottom supports an angular spectrum decomposition of the wave field as described in detail by Suh *et al.* (1990); accordingly we write the free wave field as a summation of plane waves:

$$\begin{bmatrix} \Phi^{(1)} \\ \eta^{(1)} \end{bmatrix} = \sum_{n=2}^{\infty} \gamma^n \sum_{p=-\infty}^{\infty} \sum_{q=-\infty}^{\infty} \begin{bmatrix} \phi_{p,q}^{(n,1)} \\ \zeta_{p,q}^{(n,1)} \end{bmatrix} E_{p,q}, \tag{6}$$

where $\left\{\phi_{p,q}^{(n,1)}, \zeta_{p,q}^{(n,1)}\right\}$ are complex amplitudes of free wave components of order γ^n with angular frequency $\omega_p = p\omega$ and alongshore wavenumber $\lambda_q = q\lambda$, with ω and λ representing the discrete frequency and alongshore wavenumber spacing. Note that the expansion parameter is γ (not ϵ) to prevent fractional powers and the summation over n accordingly starts at 2 (not at 1); it should be kept in mind though that $O(\gamma^2) = O(\epsilon)$.

The $E_{p,q}$ capture the rapid phase variations according to

$$E_{p,q} = \exp\left[i\chi_{p,q}\right], \quad \chi_{p,q} = \int^x \mathbf{k}_{p,q} \cdot \mathbf{dx} - \omega_p t = \int^x \varkappa_{p,q}\, dx + \lambda_q y - \omega_p t, \tag{7}$$

where $\varkappa_{p,q} = \sqrt{k_p^2 - \lambda_q^2}$ and k_p is related to the angular frequency, ω_p, through the linear dispersion relation $\omega_p^2 = gk_p \tanh(k_p\overline{h})$. In addition to the free wave components which evolve due to (near-)secular wave-wave and wave-bottom interactions, we also consider bound waves resulting from non-resonant quadratic interactions, which require a special treatment in the shallow water limit where the mismatch from resonance vanishes. The total wave field can be expressed as:

$$\begin{bmatrix} \Phi \\ \eta \end{bmatrix} = \sum_{n=2}^{\infty} \gamma^n \left\{ \sum_{\mathbf{v}_1} \begin{bmatrix} \phi_1^{(n,1)} \\ \zeta_1^{(n,1)} \end{bmatrix} E_1 + \gamma^2 \sum_{\mathbf{v}_1,\mathbf{v}_2} \begin{bmatrix} \phi_{1,2}^{(n+2,2)} \\ \zeta_{1,2}^{(n+2,2)} \end{bmatrix} E_{1,2} \right\} + \text{H.B.C..} \tag{8}$$

Here H.B.C. denotes Higher-order Bound Components (of sixth and higher order in γ) that will not be considered in our analysis. For notational convenience we introduced $E_{1,2} = E_1 E_2$ and we combined the summation over frequencies and alongshore wavenumber by a summation over all permutations of the vector, $\mathbf{v}_1 = \{\lambda_1, \omega_1\}$; the numerical subscripts refer to the vector, $\mathbf{v}$ correspondingly subscripted. To quantify the mismatch from exact quadratic resonance we consider a normalized cross-shore wavenumber difference as in

$$\mu = \frac{\varkappa_1 + \varkappa_2 - \varkappa_{1+2}}{\varkappa_{1+2}}. \tag{9}$$

Whereas the traditional Stokes expansion is valid only in deep-intermediate water depths where $\mu = O(1)$, an alternative treatment of bound waves is presented here which extends the validity to relatively shallow water where μ is of the same order as the nonlinearity parameter ϵ (or $O(\mu) = O(\gamma^2)$ in the present scheme), which corresponds to the classic Boussinesq approximation.

3. The amplitude evolution model

Based on the assumptions outlined in §3 and by introducing multiple scales (see e.g. Liu & Dingemans, 1989; Suh *et al.*, 1990) a cascade of solutions to the boundary value problem (1) in increasing order of γ can be obtained, where the effects of the weak two-dimensionality and nonlinearity are incorporated as modulations of the complex spectral amplitudes. Note that the lateral variations of the wave field and water depth are captured in x-dependent Fourier coefficients; as a consequence, the two-dimensional wave field evolution is described by a set of ordinary differential equations

in x. The details of the expansion, including quadratic near-resonances, are presented in JHB. Here we simply state the resulting evolution equation and give a heuristic derivation to include quadratic near-resonances in the shallow water limit.

3.1. *Deep to intermediate water depth, $O(\mu) = O(1)$*

To $O(\gamma^4)$, a one-dimensional evolution equation for the spatial variations of the spectral amplitudes, $\zeta_1^{(2,1)}$, results,

$$\mathcal{T}_1\{\zeta_1^{(2,1)}\} = \xi_1^{(\mathrm{wb})} + \xi_1^{(\mathrm{wbb})}, \qquad \mathcal{T}_1\{\} = \left(d_x + \frac{d_x V_1}{2V_1}\right), \tag{10}$$

which is accurate over distances $O(k_0^{-1}\gamma^2)$. Here d_x is a shorthand for $\frac{d}{dx}$ and $V_1 = \frac{\varkappa_1}{k_1} C_{g,1}$ is the cross-shore component of the group speed vector in the linear approximation. The forcing terms $\xi_1^{(\mathrm{wb})}$ and $\xi_1^{(\mathrm{wbb})}$ incorporate quadratic and cubic interactions of the surface waves with the residual depth; both are linear in the surface elevation while linear and quadratic in the bottom perturbation, respectively. Explicit expressions of $\xi_1^{(\mathrm{wb})}$ and $\xi_1^{(\mathrm{wbb})}$ are given in the Appendix A; differences with expressions in Suh *et al.* (1990) are addressed in JHB.

Since the linear dispersion relation does not support secular forcing terms due to quadratic wave-wave interactions (e.g. Phillips, 1977), these interactions generally result in components with *bounded* $O(\gamma^4)$ (in the present scaling) amplitudes that are ***phase coupled*** to the primary waves. The component amplitudes, $\zeta_{1,2}^{(4,2)}$, read

$$\zeta_{1,2}^{(4,2)} = \frac{\mathcal{Z}_{1,2}}{\Delta_{1,2}} \zeta_1^{(2,1)} \zeta_2^{(2,1)}, \tag{11}$$

which agrees with expressions in Hasselmann (1962) and where

$$\mathcal{Z}_{1,2} = \frac{\omega_{1,2}}{\omega_1 \omega_2} \left(\mathcal{D}_{1,2} + \frac{g\Delta_{1,2}}{\omega_{1,2}} \mathcal{R}_{1,2} \right), \qquad \Delta_{1,2} = k_{1,2} T_{1,2} - \frac{\omega_{1+2}^2}{g}. \tag{12}$$

The interaction coefficients are given in Appendix B and we use the shorthands

$$k_{1,2} = |\mathbf{k}_1 + \mathbf{k}_2|, \quad \omega_{1,2} = \omega_{1+2} = \omega_1 + \omega_2, \quad T_{1,2} = \tanh k_{1,2}\overline{h}. \tag{13}$$

3.2. *A heuristic extension to shallow water, $O(\mu) = O(\gamma^2)$*

As the water depth decreases such that $O(\mu) \to O(\gamma^2)$ the denominator in (11) becomes $O(\gamma^2)$ and the notion of quadratic wave-wave interactions resulting in bound components of higher order no longer holds.

Instead these interactions approach resonance with concomitant leading-order, cross-spectral energy transfers over distances $O(k_0^{-1}\gamma^2)$. A formal extension of the perturbation expansion to include this transition from bound wave motion to near-resonant quadratic wave-wave interactions is described in JHB. Here we consider a more heuristic approach: Note that as $O(\mu) \to O(\gamma^2)$ the distinction between free and bound components is no longer obvious as the quadratic wave-wave forcing terms become secular. Therefore we anticipate that – in that limit – the amplitude $\zeta_{1,2}^{(4,2)}$ undergoes modulations due to the interaction with the topography described by $\mathcal{T}_{1+2}\{\zeta_{1,2}^{(4,2)}\} = \xi_{1+2}^{(\mathrm{wb})} + \xi_{1+2}^{(\mathrm{wbb})}$ with the forcing terms being equal to those in the *RHS* of (10) but with $\zeta_1^{(2,1)}$ consistently replaced by $\zeta_{1,2}^{(4,2)}$. We incorporate the bound wave components as modulations of the free wave amplitudes and introduce a composite amplitude

$$\widehat{\zeta}_1 = \gamma^2\zeta_1^{(2,1)} + \gamma^4 \sum_{\mathbf{v_2}+\mathbf{v_3}=\mathbf{v_1}} \zeta_{2,3}^{(4,2)} E_{2,3;1} \tag{14}$$

with $E_{2,3;1} = E_2 E_3 E_1^*$. Applying the operator $\mathcal{T}_1\{\}$ on $\widehat{\zeta}_1$ yields

$$\mathcal{T}_1\{\widehat{\zeta}_1\} = \widehat{\xi}_1^{(\mathrm{wb})} + \widehat{\xi}_1^{(\mathrm{wbb})} + i\gamma^4 \sum_{\mathbf{v_2}+\mathbf{v_3}=\mathbf{v_1}} \Lambda_{2,3}\zeta_{2,3}^{(4,2)} E_{2,3;1}. \tag{15}$$

Here $\Lambda_{2,3} = \varkappa_2 + \varkappa_3 - \varkappa_{2+3}$ and the forcing terms $\widehat{\xi}_1^{(\mathrm{wb})}$ and $\widehat{\xi}_1^{(\mathrm{wbb})}$ are equal to those in the *RHS* of (10) but with $\zeta_1^{(2,1)}$ replaced by $\widehat{\zeta}_1$. The last term in the *RHS* of (15) incorporates the modulations due to quadratic wave interactions. Upon further replacing $\zeta_{2,3}^{(4,2)}$ in that term by the expression (11) and the product $\gamma^4\zeta_2^{(2,1)}\zeta_3^{(2,1)}$ by $\widehat{\zeta}_2\widehat{\zeta}_3$, which is consistent to the order retained in the equations, we obtain the transport equation:

$$\left(d_x + \frac{d_x V_1}{2V_1}\right)\widehat{\zeta}_1 = \widehat{\xi}_1^{(\mathrm{wb})} + \widehat{\xi}_1^{(\mathrm{wbb})} + i \sum_{\mathbf{v_2}+\mathbf{v_3}=\mathbf{v_1}} \frac{\Lambda_{2,3}}{\Delta_{2,3}} \mathcal{Z}_{2,3}\widehat{\zeta}_2\widehat{\zeta}_3 E_{2,3;1}. \tag{16}$$

Equation (16) is the final result of the present analysis; the first two forcing terms on the *RHS* describe the effects of the two-dimensional topography; the last foring term incorporates quadratic wave nonlinearity for arbitrary resonance mismatch and is accurate from deep-intermediate water depth (Stokes limit) to shallow water (Boussinesq limit). Even though the model describes wave evolution in two dimensions, it should be noted that (16) is a coupled set of ordinary differential equations. This approach has the advantage over traditional refraction-diffraction models (that solve a two-dimensional transport equation) that numerical implementations are relatively simple. The reduction from a partial to an ordinary differential

equation comes at the expense of additional quadratic and cubic forcing terms that incorporate the effects of weak lateral depth variations through the scattering of energy between alongshore wavenumber components.

For one-dimensional wave propagation (16) is equivalent to equation (19) in Bredmose *et al.* (2002) (note that the operator $H(h_0\nabla, k_p h_0)$ in Bredmose *et al.* is equivalent to $i\frac{\Lambda_{p1,p2}}{\Delta_{p1,p2}}$). For near-resonant quadratic wave-wave interactions (implying $\Delta_{1,2} = 2g^{-1}\omega_{1+2}V_{1+2}\Lambda_{1,2} + O(\mu^2)$) over alongshore-uniform topography (16) reduces to the deterministic expressions in Sheremet (1996) and Eldeberky & Madsen (1999) while in shallow water (Boussinesq limit) it is equivalent to Herbers & Burton (1997).

4. Comparison to experimental data

In this section we compare the numerical evaluation of expression (16) to experimental data, both to verify the accuracy of the weak-2D approximation and the combined effect of propagation over two-dimensional topography with harmonic generation in shallow water. In the numerical simulations we compute the evolution of three frequency components (primary, first and second harmonic). The numerical integration of (16) is performed using a standard, fourth-order, fixed step-size, Runge-Kutta scheme, with spatial step size $\Delta x = 0.05\,\mathrm{m}$. We consider only propagating modes and neglect evanescent mode motion.

4.1. *Wave focusing over a circular shoal*

The experimental set-up reported by Chawla *et al.* (1996) is shown in Figure 1. It consists of a circular shoal placed on an otherwise horizontal bottom. The water depth in the horizontal area around the shoal is 0.45 m while at the center of the shoal it measures 0.08 m. Wave gauges are aligned with the transects $A - A'$ through $G - G'$. The incident wave field propagates in positive x direction (see Figure 1), with frequency $f = 1.0\,\mathrm{Hz}$ and wave height $H = 0.0233\,\mathrm{m}$. The wave field experiences strong two-dimensional effects induced by the topography, including a strong focal region behind the shoal where combined effects of refraction and diffraction are important. Nonlinearity for this case is very weak.

A comparison between model results (viz. eq. (16)) and observations along four transects ($A - A'$, $B - B'$, $C - C'$ and $D - D'$) is shown in Figure 2. The wave height variations along $A - A'$ are accurately predicted by the model, including the strong increase over the shoal and decrease for $x > 10\,\mathrm{m}$. Not all the details of the lateral wave height variation are

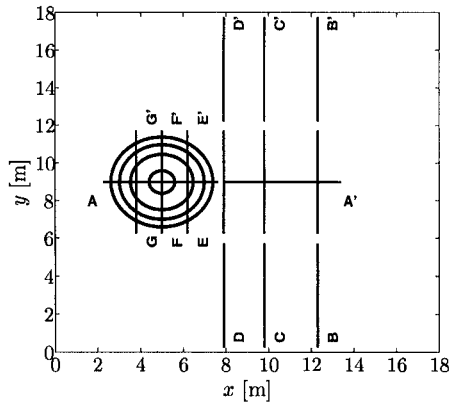

Figure 1. Depth contours wave basin reported in Chawla *et al.* (1996). Wave gauges are aligned with transects $A - A'$ through $G - G'$ indicated in figure.

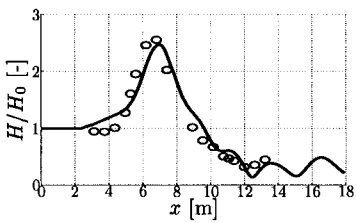

(a) Transect A-A', $y = 9.0$ m

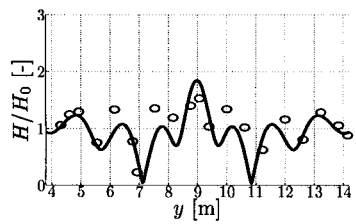

(b) Transect D-D', $x = 7.9$ m

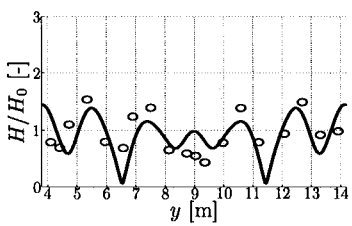

(c) Transect C-C', $x = 9.8$ m

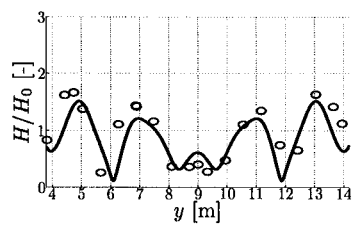

(d) Transect B-B', $x = 12.3$ m

Figure 2. Comparison computed and observed normalized wave height along transects. Solid line and circles denote model result and observations by Chawla *et al.* (1996) respectively.

resolved along $C - C'$ and $D - D'$ but overall the simulations are in good agreement with the observations.

4.2. *Harmonic generation over a convex beach*

Whalin (1971) performed experiments on an alongshore convex-shaped beach. Here we compare model predictions to observations of a periodic wave field normally incident with frequency $f = 0.5\,\text{Hz}$ and wave height $H = 0.0212\,\text{m}$. To illustrate the nature of the wave transformation on the topography, Figure 3 shows a snapshot of a simulated surface elevation for this case, superposed on the bathymetry. Water depth varies from 0.45 m to 0.15 m and waves enter from the deeper end of the tank. The experimental set-up includes a focal region where the combined effects of refraction, diffraction and strong enhancement of harmonics are important.

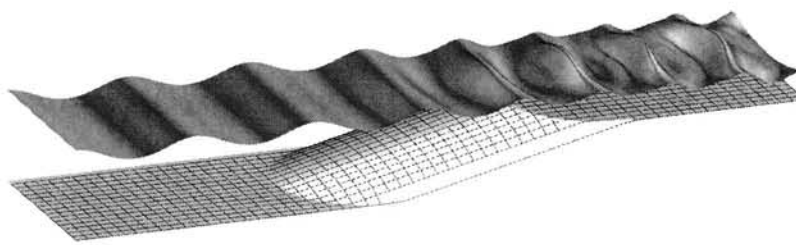

Figure 3. Snapshot of simulated surface elevation of a wave field with frequency $f = 0.5\,\text{Hz}$ and wave height $H = 0.0212\,\text{m}$ propagating over bathymetry reported by Whalin (1971). Waves propagate from left to right.

Figure 4 shows the comparison between observations and model predictions of the spatial evolution of amplitudes of the primary, first and second harmonics. The discrepancies noted for the first and second harmonics between $x = 5\,\text{m}$ and $x = 10\,\text{m}$ are likely due to the presence of spurious wave motion in the observations (e.g. due to inaccuracies in the wave generation, see Whalin, 1971) not present in the simulation; the enhancement of these harmonics in the nearshore region is accurately predicted. Overall, apart from the computed oscillations of the primary harmonic, which is not present in the observations (a similar discrepancy was invariably found by other authors, see e.g. Kaihatu & Kirby, 1995; Tang & Ouellet, 1997), the model predictions compare very favorably to the observed evolution of the harmonics.

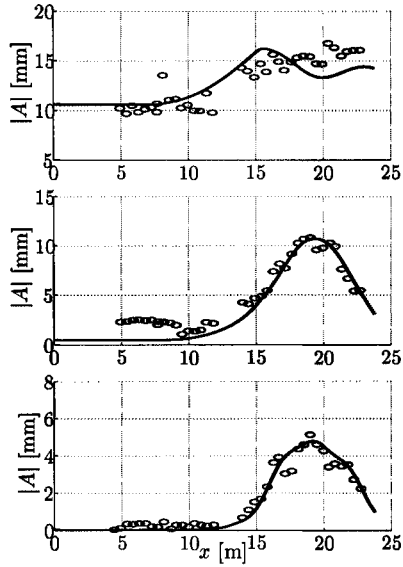

Figure 4. Evolution absolute values wave amplitudes for wave propagation over bathymetry reported by Whalin (1971); $f = 0.5\,\mathrm{Hz}$ and $H = 0.0212\,\mathrm{m}$. Top, middle and bottom panel show comparison for primary, first and second harmonic respectively. Circles denote observed values, solid line represents model result.

5. Conclusions

A discrete spectral model for wave propagation over weakly two-dimensional topography is presented. The model accounts for the combined effects of shoaling, refraction, diffraction and quadratic nonlinear interactions for arbitrary resonance mismatch. The evolution of the spectral amplitudes is described by a coupled set of first-order, ordinary differential equations. Comparison of simulations to experimental data shows that: 1) the model is capable of accurately predicting wave field evolution over two-dimensional topography, 2) enhancement of harmonics over two-dimensional topography is in good agreement with observed evolution of harmonic amplitudes.

Acknowledgments

This research is supported by the Technology Foundation STW, applied science division of NWO and the technology programme of the Ministry of Economic Affairs in the Netherlands, under project number DCB.6025. THCH is supported by the Office of Naval Research and the National Sci-

ence Foundation in the USA. We gratefully acknowledge James Kaihatu for providing digital data from the Whalin experiment and Ole Sørensen for generously providing a copy of the corresponding report. We thank Marcel Zijlema for kindly sharing his preprocessing efforts of the experimental data reported by Chawla *et al.* (1996) and Arun Chawla for granting the use of the data in this paper.

Appendix A. Forcing terms lateral depth variations

The forcing terms on the transport equation in (10) read

$$\xi_1^{(\mathrm{wb})} = i\left(1-T_1^2\right)\frac{g}{2\omega_1 V_1}\Big[k_1^2\mathcal{G}_1\{\widetilde{h},\zeta_2^{(2,1)}\} - \mathcal{G}_1\{\widetilde{h}_x, i\varkappa_2\zeta_2^{(2,1)}\} - \mathcal{G}_1\{\widetilde{h}_y, i\lambda_2\zeta_2^{(2,1)}\}\Big] \tag{A.1a}$$

$$\xi_1^{(\mathrm{wbb})} = i\left(1-T_1^2\right)\frac{g}{2\omega_1 V_1} * \mathcal{G}_1\{\widetilde{h}, \frac{C_1}{2C_{g,1}}k_1^3\frac{\left(1-T_1^2\right)}{T_1}\left(2-\frac{k_1^2P_1}{\varkappa_1}+\frac{T_1^2}{\left(1-T_1^2\right)}\right)\mathcal{G}_2\{\widetilde{h},\zeta_3^{(2,1)}\}\}. \tag{A.1b}$$

Here $T_1 = \tanh k_1\overline{h}$, $C_1 = \frac{\omega_1}{k_1}$ and

$$P_1 = \frac{1}{2V_1}\left[\left(1-\left(\frac{\varkappa_1}{k_1}\right)^2\right)\frac{C_{g,1}}{k_1}+\frac{g\overline{h}}{\omega_1}\left(\frac{\varkappa_1}{k_1}\right)^2\right]. \tag{A.2}$$

The operator

$$\mathcal{G}_i\{a,b_j\} = \mathcal{F}_i\{a\mathcal{F}^{-1}\{b_j e^{i\psi_j}\}\}e^{-i\psi_i} \tag{A.3}$$

with $\mathcal{F}_i$ and $\mathcal{F}^{-1}$ denoting the i^{th} component of the Discrete Fourier Transform (DFT) with respect to the lateral coordinate and the Inverse DFT respectively, the $\psi_i = \int^x \varkappa_i dx'$. Note that a is a function of the lateral coordinate.

Appendix B. Quadratic wave-wave interaction coefficients

$$\mathcal{D}_{1,2} = -\frac{1}{2}\Big[\omega_1 k_2^2\left(1-\frac{\omega_2^2}{gk_2}T_2\right)+\omega_2 k_1^2\left(1-\frac{\omega_1^2}{gk_1}T_1\right) -2\left(\omega_1+\omega_2\right)\left(k_1k_2T_1T_2-\mathbf{k}_1\cdot\mathbf{k}_2\right)\Big] \tag{B.1}$$

$$\mathcal{R}_{1,2} = \frac{1}{2g}\left[\omega_1\omega_2\left(k_1T_1+k_2T_2\right)+g\left(k_1k_2T_1T_2-\mathbf{k}_1\cdot\mathbf{k}_2\right)\right] \tag{B.2}$$

References

AGNON, Y., A. SHEREMET, J. GONSALVES AND M. STIASSNIE. 1993. Nonlinear evolution of a unidirectional shoaling wave field, *Coast. Eng.*, **20**, 29–58.

ARDHUIN, F. & T.H.C. HERBERS. 2002. Bragg scattering of random surface gravity waves by irregular sea bed topography, *J. Fluid Mech.*, **451**, 1–33.

BOCZAR-KARAKIEWICZJI, B. & R.G.D. DAVIDSON-ARNOTT. 1987. Nearshore bar formation by non-linear wave processes - a comparison of model results and field data, *Marine Geology*, **77**, 287–304.

BREDMOSE, H., P.A. MADSEN, H.A. SCHÄFFER AND Y. AGNON. 2002. Fully dispersive evolution equations: wave breaking and efficiency, *Proc. 28th Int. Conf. Coastal Eng.*, 281–292.

BYRNE, R.J. 1969. Field occurences of induced multiple gravity waves, *J. Geoph. Res.*, **74**(10), 2590–2596.

CHAWLA, A. H., H. T. OZKAN-HALLER AND J. T. KIRBY. 1996. Experimental study of breaking waves over a shoal, *Proc. 25th Int. Conf. Coastal Eng.*, 2–15.

ELDEBERKY,Y. & P.A. MADSEN. 1999. Deterministic and stochastic evolution equations for fully dispersive and weakly nonlinear waves, *Coast. Eng.*, **38**, 1–24.

FREILICH, M.H. & R.T. GUZA. 1984. Nonlinear effects on shoaling surface gravity waves, *Proc. Roy. Soc. Lond. A*, **311**, 1–41.

HASSELMANN, K. 1962. On the non-linear energy transfer in a gravity-wave spectrum, *J. Fluid Mech.*, **49**, 481–500.

HERBERS, T.H.C. & M.C. BURTON. 1997. Nonlinear shoaling of directionally spread waves on a beach, *J. Geoph. Res.*, **102**, 21,101–21,114.

JANSSEN, T.T., T.H.C. HERBERS AND J.A. BATTJES. 2004. Generalized evolution equations for nonlinear surface gravity waves over weak-2D topography, *To be submitted.*

KAIHATU, J.M. & J.T. KIRBY. 1995. Nonlinear transformation of waves in finite water depth, *Phys. Fluids*, **7**, 1903–1914.

LIU, P.L.-F. & M.W. DINGEMANS. 1989. Derivation of the Third-order evolution equations for weakly nonlinear water waves propagating over uneven bottoms, *Wave motion*, **11**, 41–64.

MADSEN, P.A. & H.A. SCHÄFFER. 1998. Higher-order Boussinesq-type equations for surface gravity waves:derivation and analysis, *Proc. Roy. Soc. Lond. A*, **356**, 3123–3184.

MADSEN, P.A. & O.R. SØRENSEN. 1993. Bound waves and triad interactions in shallow water, *Ocean Eng.*, **20**, 4, 359–388.

MUNK, W.H. 1949. Surf beats, *Eos Trans. AGU*, **30**, 849–854.

MUNK, W.H. & M.A. TRAYLOR. 1949. Refraction of ocean waves: A process linking underwater topography to beach erosion, *J. of Geology*, **LV**, 1–26.

PHILLIPS, O.M. 1977. The Dynamics of the Upper Ocean, *Cambr. Univ. Press*, 2nd edition, 359–384.

RAYLEIGH, A.M. 1876. On waves, *Phil. Mag.*, **1**, 4, 257–279.

SHEREMET, A. 1996. Wave interaction in shallow water, ScD thesis, Technion, Haifa, Israel, 99 p.

SUH, K.D., R.A. DALRYMPLE AND J.T. KIRBY. 1990. An angular spectrum model for propagation of Stokes waves, *J. Fluid Mech.*, **221**, 205–232.

TANG, Y & Y. OUELLET. 1997. A new kind of nonlinear mild-slope equation for combined refraction-diffraction of multifrequency waves, *Coast. Eng.*, **31**, 3–36.

WHALIN, R.W. 1971. The limit of application of linear wave refraction theory in a convergence zone, *Res. Rep. No. H-71-3,*, U.S. Army Engineer Waterways Experiment Station, Vicksburg, MS, 156 p.